Laboratory Investigations

An Examination of Triassic Cynodont Tooth Enamel Chemistry Using Fourier Transform Infrared Spectroscopy

J. Botha,[1] **J. Lee-Thorp,**[2] **M. Sponheimer**[3]

[1]Karoo Palaeontology, Natural History Division, South African Museum, Iziko Museums of Cape Town, Cape Town, South Africa
[2]Archaeometry Research Unit, University of Cape Town, Rondebosch, Cape Town, South Africa
[3]Department of Biology, University of Utah, Salt Lake City, UT 84112, USA

Abstract. The Cynodontia are considered to be particularly significant as their remains document the reptile-to-mammal transition during the Permian and Triassic periods. Studies examining cynodont morphology and anatomy have shown that these animals acquired increasingly mammal-like characteristics during their evolution. In this study, we use Fourier Transform Infrared spectroscopy to assess the enamel structure of several Triassic cynodonts. Extant *Crocodylus niloticus* and *Varanus* enamel spectra as well as published extant and fossil mammalian data were used as comparisons. The profiles of the cynodont spectra resemble biological apatite, in spite of their great age. The ratio of structural carbonate to phosphate in these cynodonts is significantly higher than in the extant and fossil mammals, but very similar to the extant reptiles. We suggest that the enamel apatite structure of these cynodonts was more similar to the reptilian rather than the mammalian pattern.

Key words: Tooth — Enamel — Therapsid — Cynodont — Fourier Transform Infrared spectroscopy

The Cynodontia are considered to be the best-documented example in the fossil record of an evolutionary sequence connecting two major structural grades, namely, the reptiles and the mammals [1]. The Cynodontia first appeared during the end of the Late Permian period [2], approximately 253 million years ago (Smith, personal communication). Their remains have been recovered from Russia, China, India, North and South America, western Europe, Antarctica, Tanzania, and Zambia [3]. However, the most complete cynodont fossil record is found in the Karoo Basin of South Africa.

The cynodonts have received much attention as it is currently thought that they are the ancestors of extant mammals. Most studies have focused on the macroscopic aspects of these animals, such as their skeletal morphology and functional anatomy [3, 4]. These studies have provided significant information about their locomotion, biomechanical adaptations, and phylogeny, indicating that cynodonts have morphological characteristics found in both reptiles and mammals [3–7]. For example, the cynodont posture consisted of a sprawling forelimb, similar to reptiles and a more mammal-like semi-erect hindlimb [3, 4, 8]. Reduced lumbar rib structure and a secondary bony palate, which are mammalian characteristics, have also been found in the later cynodonts, indicating that they developed more mammal-like features as they became more derived [4]. In addition, bone microstructural studies have revealed that cynodont growth patterns also exhibit features present in both reptiles and mammals. For instance, the bone histology of the derived cynodont *Diademodon* consists of rapidly forming fibrolamellar bone generally found in extant mammals, alternating with growth rings usually found only in extant reptiles [9].

Dental morphology reveals further information regarding tooth wear, mastication, and jaw function [10–13]. *Diademodon*, for example, is considered to be one of the first cynodonts to exhibit a combination of a mammal-like jaw adductor musculature and precise postcanine occlusion [11, 12]. However, fewer studies have focused on dental microstructure [14–16] and no studies have analyzed the crystalline chemistry of cynodont enamel apatite to ascertain whether it might resemble that of mammals. This may not necessarily be the case as Grine et al. [14], using scanning electron microscopy, found that *Diademodon* lacked the prismatic enamel structure typical of mammals. The enamel structure of

---

Correspondence to: J. Botha; E-mail: jbotha@iziko.org.za
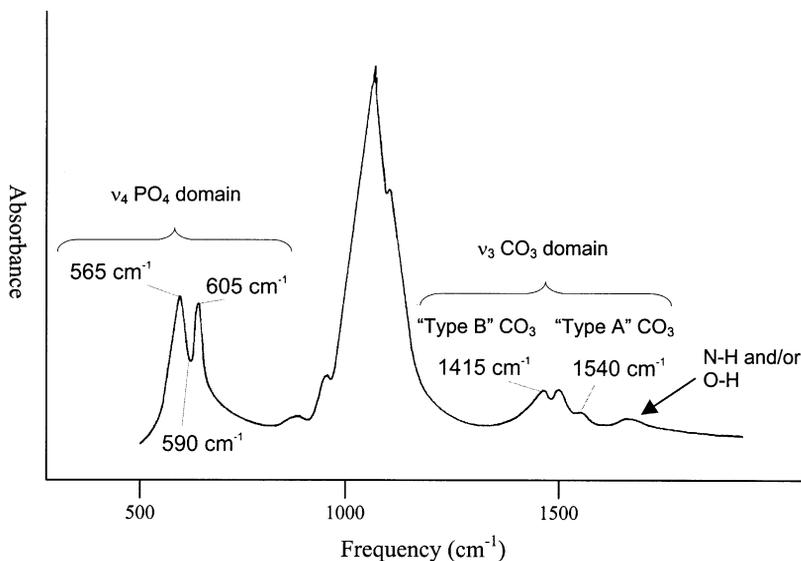
Fig. 1. Typical extant mammalian (*Giraffa camelopardalis*) FTIR absorbance spectrum of a biological apatite showing the phosphate (565 cm^{-1}, 605 cm^{-1}, and 590 cm^{-1}) and carbonate peaks (1415 cm^{-1} and 1540 cm^{-1}). The sample was prepared following the techniques used for the study material. The arrow indicates an N—H and/or O—H peak at 1640 cm^{-1}.

derived cynodonts such as *Diademodon* is now referred to as synapsid columnar enamel, whereas that of the early Mesozoic mammals such as *Megazostrodon* is known as plesiomorphic prismatic enamel [15].

Tooth enamel is compact with little pore space and contains larger apatite crystals compared to dentine or bone [17]. It is therefore more resistant to physical and chemical alteration during fossilization, making it the ideal material to use for chemical analyses on fossil material.

In this study, nonmammalian cynodont tooth enamel of Early to Middle Triassic age was examined in order to assess the nature of the biological apatite. Measures such as nuclear magnetic resonance, scanning and transmission electron microscopy, and Fourier Transform Infrared (FTIR) spectroscopy [17] can be used to assess the chemistry, substitutions, and crystallinity of extant material. In FTIR spectroscopy, the functional groups in biological apatites (e.g. HPO_4^{2-}, PO_4^{3-}, CO_3^{2}) absorb infrared energy at specific frequencies, which alter according to their properties and positions in the structure. FTIR spectra distinguish between enamel and bone or dentine apatites and also between major animal groups. For instance, shark tooth enamel (or enameloid) differs from that of mammals [17]. We are not aware of such characterizations of reptilian enamel.

Enamel contains carbonate substituted in at least two anionic sites. This carbonate plays an important role in affecting crystallinity and solubility of the mineral phase [17]. Most of the carbonate is substituted at the trivalent phosphate (PO_4^{3-}) sites, generally designated as "type B" carbonate, whereas a lesser amount is substituted in the monovalent hydroxyl anionic (OH$^-$) sites and is generally designated as "type A" carbonate [18] (Fig. 1). Such substitutions, especially that of CO_3^{2-} for PO_4^{3-} or CO_3^{2-} for OH$^-$, affect the dimensions of the unit cell and

change the chemical properties such as solubility and crystallinity [17].

Recent studies [19, 20] have shown that FTIR can also be used for assessing the integrity of fossil biological apatite, including enamel. It is a quick technique, which also makes minimal demands on valuable fossil material. The proportions of "type A" and "B" carbonate may alter to some extent due to fossilization resulting in another form of apatite (e.g., fluorapatite; [19–21]). However, as the absorption spectra of biological apatites differ from that of other carbonate minerals such as calcite, diagenetic minerals in fossil material can be detected [17, 20].

The genera under study, *Cynognathus*, *Diademodon*, and *Trirachodon*, are derived cynodonts, which have several mammalian morphological features such as a bony secondary palate, complex postcanine dentition, reduced lumbar ribs, and a parasagittal gait [3, 4, 22]. *Cynognathus* was a large, robust carnivorous cynodont that reached up to 2 m in length. The cranium of this animal is characterized by a long narrow snout, enlarged dentary bone, robust postorbital bar and zygomatic arch, and an unusually large squamosal. The sectorial teeth have wear-facets indicating that the teeth occluded and were probably used in a shearing action to cut up meat [4, 23–25]. *Diademodon* was a large omnivorous [13] cynodont, similar in size to *Cynognathus*. The cranium is characterised by a narrow snout, wide orbital region, and anterodorsally placed eyes [4, 26, 27]. The temporal fenestrae are large and separated from one another by a narrow, high sagittal crest [4] and the postorbital region of the zygomatic arch is unusually deep [28, 29]. *Trirachodon* was a herbivorous cynodont closely related to *Diademodon*, the main differences being a smaller body size (up to 50 cm in length) and a difference in the structure and number of the postcanine

Table 1. Localities of the study material used for FTIR spectroscopic analysis. Extant and fossil mammals were taken from [20]. All extant teeth were unweathered and well-preserved. They were taken from sub-adult and adult individuals.

Genus	Specimen number	Locality	Age[a]
Cynognathus	SAM-PK-3029 BP1 11675d	Burgersdorp	220 Ma
Diademodon	UMCZ T504a, 504b, 475	Lady Frere	220 Ma
Trirachodon	SAM-PK-5881	Aliwal North	220 Ma
Crocodylus niloticus	CROC6-CROC14	Le Bonheur Crocodile Farm, Stellenbosch	Extant
Varanus	1	University of Cape Town, Cape Town	Extant
Mammals			
Raphicerus melanotis	RAP		Extant
Syncerus caffer	BUF		Extant
Damaliscus dorcas	DOR		Extant
Papio cynocephalus	BAB		Extant
Damaliscus dorcas	DO2		Extant
Raphicerus campestris	SBK	Steenbokfontein	3 Ka
Aepyceros melampus	BC1	Border Cave	90 Ka
Hippotragus equinus	BC2	Border Cave	90 Ka
Tragelaphus oryx	FL1	Florisbad	200 Ka
Tragelaphus oryx	FL2	Florisbad	200 Ka
Connochaetes taurinus	SK1	Swartkrans	11 Ka
Antidorcas bondi	SK2	Swartkrans	11 Ka
Giraffa jumae	ML1	Makapansgat	3 Ma
Giraffa jumae	ML2	Makapansgat	3 Ma
Giraffa jumae	ML3	Makapansgat	3 Ma

[a] Ma = million years ago; Ka = thousand years ago

teeth. *Trirachodon* has fewer postcanines, which are shorter anteroposteriorly and broader transversely than *Diademodon* [4, 30]. Although cynodont morphology has been studied in depth [1, 3, 4], little is known about their enamel chemical structure and its similarities to extant animals. We use FTIR spectroscopy to assess the chemical structure of the enamel of these cynodonts for comparison with extant reptiles and mammals.

Materials and Methods

The cynodont teeth include one *Trirachodon*, two *Cynognathus*, and three *Diademodon* canines. These teeth were excavated from the *Cynognathus* Assemblage Zone, Beaufort Group, Karoo Super Group of South Africa and are of Early to Middle Triassic age (Table 1). The extant material includes nine *Crocodylus niloticus* (Nile crocodile) teeth and one *Varanus* (monitor lizard) tooth (Table 1). We used published extant and fossil mammalian enamel data [20] as comparisons, which consist of five extant (four bovid teeth, one cercopithecid tooth) and ten fossil bovid teeth (seven genera) ranging in age from 3 Ka to 3 Ma (Table 1).

As reptilian enamel is extremely thin, both enamel and dentine spectra were obtained from *Crocodylus niloticus* and *Varanus*. This was necessary in order to distinguish between the two to ensure that dentine had not been incorporated into the enamel samples.

Enamel was drilled from the outermost surface of each tooth using a low-speed, hand-held rotary drill (to prevent local heating) with a 1.5-mm diamond-tipped bit. Each 1.8-mg sample was thoroughly ground together with 300 mg of potassium bromide in an agate mortar and compressed into transparent discs under a pressure of 10 tons. The transparent FTIR discs were placed in a Perkin Elmer FT-IR Spectrometer Paragon 1000 and the resulting FTIR absorbance spectra were recorded. Sixteen scans of each sample were taken using a range of 4000–500 cm^{-1} at a resolution of 8 cm^{-1}. The spectra were downloaded to Perkin Elmer Grams Analyst 1000 (version 3.01A, Level II, 1991) where they were baseline corrected.

Peak ratios were calculated from the absorbance spectra and used to quantify changes in crystallographic structure. These ratios were calculated using the peaks of the absorption bands in the v_3 carbonate (1415 cm^{-1}, 1540 cm^{-1}) and v_4 phosphate domains (565 cm^{-1}, 590 cm^{-1}, 605 cm^{-1}) shown in Figure 1. They reflect the amount of "type B" carbonate to phosphate (BPI: 1415 cm^{-1}/605 cm^{-1}), the amount of "type A" carbonate to phosphate (API: 1540 cm^{-1}/605 cm^{-1}), the relative amount of B-to-A-site carbonate (BAI: 1415 cm^{-1}/1540 cm^{-1}), and the "crystallinity" (PCI: 565 cm^{-1}/605 cm^{-1}) of each sample [20]. Although other absorption bands can be used to assess the carbonate relationships, these bands are appropriate as they do not overlap with the absorbances of other functional groups, thus facilitating a clear examination of the A and B sites. As BPI closely tracks overall carbonate content, it was used to quantify the carbonate content in the enamel in this study, according to a relationship established by LeGeros [17].

Results

A representative FTIR spectrum from each animal group is shown in Figure 2 (please note that the y axes differ). All peak ratios, which were calculated from the
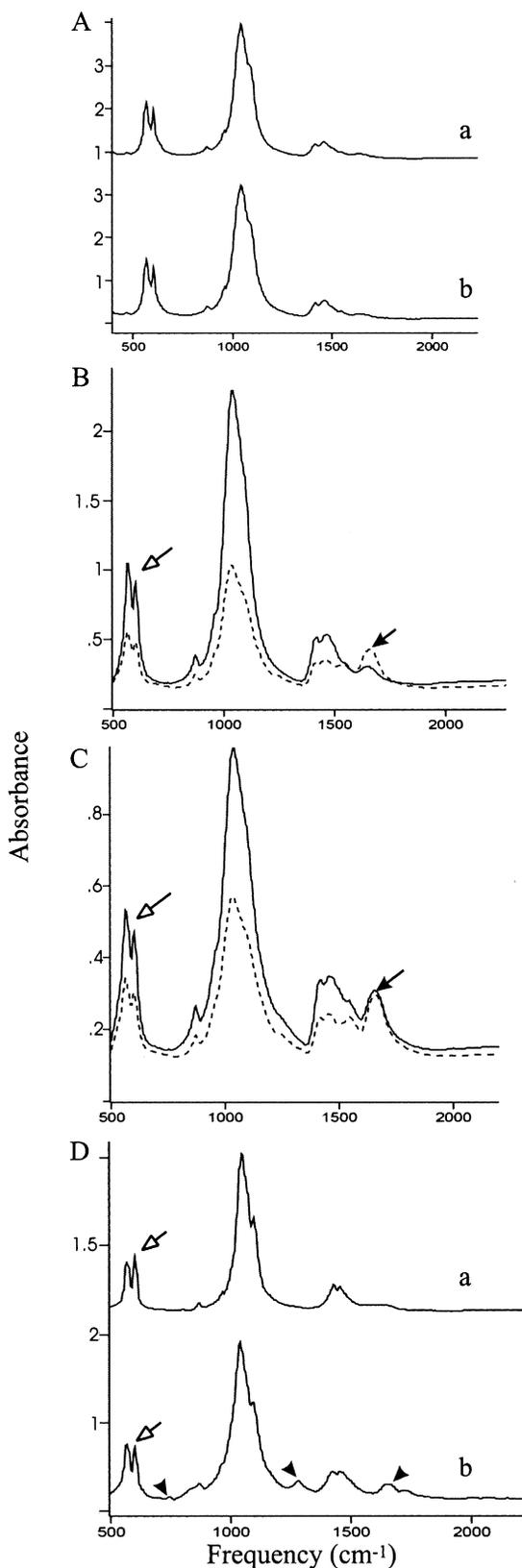
Fig. 2. FTIR spectra, including mammalian enamel, reptilian enamel and dentine, and fossil enamel spectra. (**A**) Fossil (a) and extant (b) mammal enamel. (**B**) Extant *Crocodylus niloticus* enamel (solid line) and dentine (dashed line). Open arrow indicates v_4 phosphate domain and the closed arrow indicates the 1657-cm^{-1} (N—H/O—H) peak. (**C**) Extant *Varanus* enamel (solid line) and dentine (dashed line). Open arrow indicates v_4 phosphate domain and the closed arrow indicates the 1657-cm^{-1} peak. (**D**) *Diademodon* (a) and *Trirachodon* (b) enamel. Open arrows indicate the v_4 PO$_4$ domain. Arrowheads indicate extra peaks.

Extant Mammalian versus Reptilian Enamel

When comparing the extant mammalian (Fig. 2A) and reptilian (Fig. 2B,C) enamel spectra, the reptilian spectra exhibit a lower overall absorbance in peak height, which is not due to sample mass as this was kept constant. In addition, the reptilian spectra have a higher $\sim$1657-cm^{-1} peak compared to the mammalian enamel. The $\sim$1657-cm^{-1} peak is thought to correspond to the N—H/O–H peak shown in Figure 1. Figure 3 shows a clear distinction between the reptilian and mammalian enamel. Importantly, the reptile carbonate content is significantly higher than the mammalian content (independent 1-tailed *t*-test: t_s = 10.306; df = 12; P < 0.05).

Cynodont versus Extant Enamel

The *Cynognathus* and *Diademodon* (Fig. 2D-a) enamel spectra are indistinguishable from each other and are similar in appearance to the extant *Crocodylus niloticus* spectra (Fig. 2B). In contrast, the *Trirachodon* spectrum (Fig. 2D-b) contains several extra peaks that the other two fossil spectra do not have (indicated by arrowheads in Fig. 2D-b). A notable feature of the *Cynognathus* and *Diademodon* spectra is that the 565-cm^{-1} phosphate peak in the v_4 phosphate domain has a higher absorbance than the 605-cm^{-1} phosphate peak, whereas the converse applies to the extant *Crocodylus niloticus* (Fig. 2B, open arrow) and *Varanus* (Fig. 2C, open arrow) enamel spectra. The cynodont API peak ratios are higher than both the extant and the fossil mammalian API and appear more similar to the extant reptile peak ratios. The *Diademodon* API, at 0.23, is slightly lower than the rest of the cynodont peak ratios (mean 0.36), which in turn has produced a higher BAI. The cynodont PCI results (mean 3.48) fall between the reptilian (mean 2.72) and mammalian (fossil and extant mean 0.36) peak ratios.

Figure 3 also shows that the cynodont enamel is most similar to the extant reptile enamel and is clearly distinct from the mammal enamel, both fossil and extant. The overall carbonate content is significantly different from the mammalian enamel (independent 1-tailed *t*-test: t_s = 10.871; df = 19; P < 0.05).

spectra, are given in Table 2. The BPI and BAI from Table 2 have been plotted against each other to show the similarities/differences of each group (Fig. 3).

Table 2. Peak ratios of extant and fossil enamel obtained from the FTIR absorbance spectra. The mammalian peak ratios are from [20]. The overall carbonate content ($CO_3\%_{wt}$) was estimated using the graphical relationship between BPI and carbonate percentage weight modified from [17]

Taxon	Specimen number	BPI	API	BAI	PCI	% CO3
Crocodylus niloticus	6	0.57	0.369	1.547	2.71	6.25
	7	0.577	0.316	1.826	2.764	6.25
	8	0.603	0.367	1.644	2.648	6.5
	9	0.606	0.38	1.596	2.632	6.5
	10	0.649	0.4	1.621	2.623	7
	11	0.506	0.311	1.629	2.79	5.75
	12	0.545	0.337	1.619	2.773	6
	13	0.555	0.355	1.564	2.704	6
	14	0.493	0.321	1.538	2.853	5.65
Varanus	1	0.717	0.591	1.213	2.51	7.25
Cynognathus	SAM-PK-K3029	0.6685	0.3746	1.785	3.072	7
	BP1 11675d	0.526	0.395	1.333	3.294	5.75
Diademodon	UMCZ T504a	0.533	0.207	2.575	3.892	5.75
	UMCZ T475	0.567	0.226	2.509	3.652	6
	UMCZ T504b	0.574	0.256	2.246	3.732	6.15
Trirachodon	SAM-PK-5881	0.611	0.329	1.461	3.275	6.5
Extant mammals						
Raphicerus melanotis	RAP	0.22	0.071	3.1	3.6	2.9
Syncerus caffer	BUF	0.27	0.092	2.9	3.5	3.4
Damaliscus dorcas	DOR	0.35	0.12	2.9	3.5	4.2
Papio cynocephalus	BAB	0.16	0.05	3.1	3.8	2.3
Damaliscus dorcas	DO2	0.23	0.061	3.8	3.6	3
Fossil mammals						
Raphicerus campestris	SBK	0.19	0.045	4.2	3.7	2.6
Aepyceros melampus	BC1	0.24	0.043	5.6	3.7	3.1
Hippotragus equinus	BC2	0.22	0.046	4.8	4.1	2.9
Tragelaphus oryx	FL1	0.34	0.086	4	3.4	4.1
Tragelaphus oryx	FL2	0.25	0.072	3.5	3.6	3.2
Connochaetes taurinus	SK1	0.34	0.09	3.8	3.6	4.1
Antidorcas bondi	SK2	0.33	0.09	3.7	3.4	4
Giraffa jumae	ML1	0.26	0.066	4	3.5	3.3
Giraffa jumae	ML2	0.25	0.075	3.3	3.7	3.2
Giraffa jumae	ML3	0.23	0.055	4.2	3.7	3

Reptile Enamel Versus Dentine

The enamel spectra of *Crocodylus niloticus* (Fig. 2B) and *Varanus* (Fig. 2C) are easily distinguishable from their respective dentine spectra (dashed lines) as the peaks in the enamel spectra are generally higher than the dentine peaks. Furthermore, the dentine $\sim$1657-cm^{-1} absorbance peaks are proportionately higher than the rest of the peaks in the v_3 carbonate domain compared with the respective enamel peaks.

Discussion

The profiles of the cynodont spectra resemble biological apatite in spite of the great age of the enamel. The apatite structure is only slightly altered, although it is recognized that some ionic shifts and probably recrystallization must have occurred.

Extant Enamel

The *Crocodylus niloticus* and *Varanus* $\sim$1657-cm^{-1} dentine peaks are proportionately higher than the enamel spectra, further indicating that dentine has a higher organic content than does enamel, as shown in earlier studies [17]. If this difference is noted in extant taxa, results obtained from fossil dentine may be very different from fossil enamel. Caution is therefore advised when making deductions from fossil dentine.

Although great care was taken in drilling merely the outer surface of the *Varanus* tooth to obtain enamel, the *Varanus* FTIR spectrum (Fig. 2C) shows that a small amount of dentine is likely to have been incorporated (shown by the high $\sim$1657-cm^{-1} peak). The *Crocodylus niloticus* and *Varanus* enamel and dentine are the same color and do not exhibit any observable visual differences, which poses a difficulty in distinguishing them
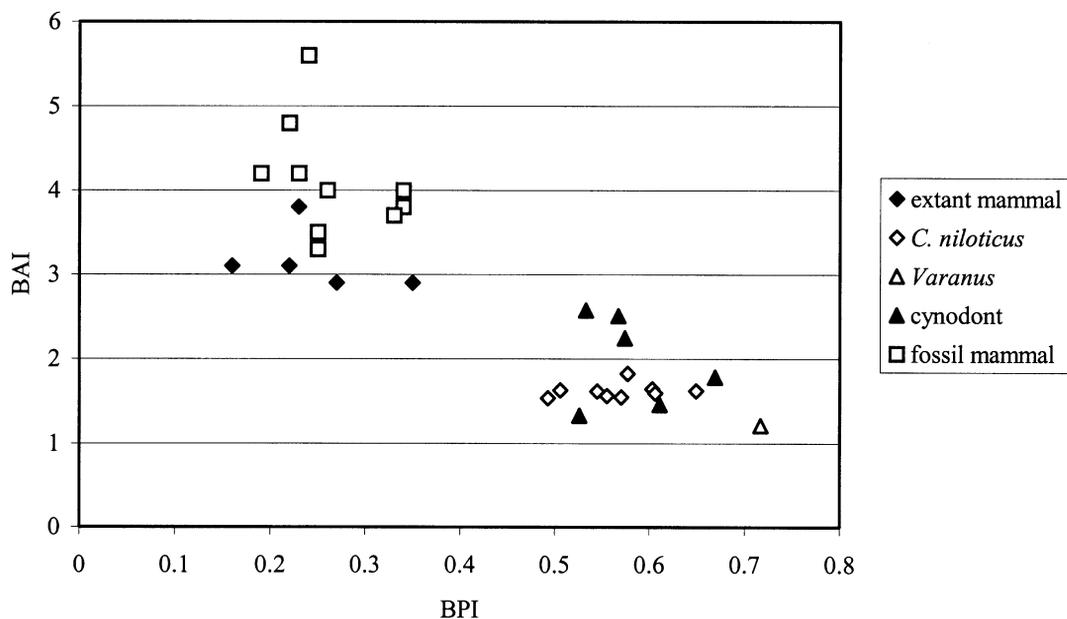
Fig. 3. BPI versus BAI of the cynodonts, extant *Crocodylus niloticus*, *Varanus*, and extant and fossil mammalian peak ratios from Sponheimer and Lee–Thorp [20].

when drilling (this differs from mammals, which have notably thicker enamel compared with reptiles). However, even relatively small amounts of dentine could be detected in the FTIR spectra. Using this criterion, it can be seen that dentine may have been incorporated into the *Varanus* sample, which may have increased the overall carbonate content as the CO_3 percentage is slightly higher than any of the other samples in the study (see Table 2).

The absorbance spectra give an overall profile of the apatite structure, but the peak ratios allow observed variations to be quantified. The extant mammalian BPI peak ratios from Sponheimer and Lee-Thorp [20] differ from the reptilian peak ratios in this study (Fig. 3). The mean reptile BPI is 0.58, whereas the mean extant mammal peak ratio is 0.25. Figure 3 shows the clear distinction between the extant mammal and reptile enamel. It is also evident that the mammal enamel has a significantly higher BAI than the reptile enamel (independent 1-tailed *t*-test: $t_s = 12.234$; $df = 12$; $P < 0.05$).

Extant versus Fossil Mammalian Enamel

The extant and fossil mammalian spectra are similar (Fig. 2A), and Figure 3 shows that the two data sets group together. The fossil and extant mammalian spectra are virtually indistinguishable to the naked eye, but the fossil API peak ratios appear to be slightly lower than that of the extant mammals. The fossil BAI is slightly higher than the extant mammal BAI but the difference is not significant. Three fossil mammal PCI values also fall outside the extant

mammal range. However, analyses of variance show that the BPI, API, and PCI of both groups do not differ significantly. There is also no significant difference in overall carbonate content between the two groups (see [20]).

According to Sponheimer and Lee–Thorp [20], the fossil mammalian enamel apatite has been altered slightly during fossilization as shown by the increase in BAI compared to the extant mammal values. They suggest that a relative increase in B-site versus A-site carbonate ions usually characterizes fossilization.

Cynodont Enamel

The overall profile of the fossil spectra, apart from that of *Trirachodon*, resembles biological apatite, suggesting that diagenesis is minimal. Diagenesis of the *Trirachodon* enamel appears to be more extensive, as shown by the extra peaks in the spectrum. In comparing the extant and cynodont enamel, the ratio between the 565-cm^{-1} and 605-cm^{-1} phosphate peaks in the v_4 phosphate domain differ (apart from *Trirachodon*). This indicates that the phosphate in the fossil material has been altered to some extent over the past ~220 million years. Phosphate is most widely used in paleontological isotope studies as it is thought to be less susceptible to diagenesis compared to carbonate. However, this is not necessarily the case, as is evident by the changes in phosphate in the v_4 phosphate domain. The *Trirachodon* spectrum is distinct from the other fossil spectra and shows how FTIR spectroscopy can be used to detect diagenesis in cynodont biological apatite.

Implications for Cynodont Biology

Both the extant and fossil mammal BPI peak ratios differ from the reptile and cynodont BPI (Fig. 3). The mean reptile BPI is 0.58 and the mean cynodont BPI is 0.57. In contrast, the extant mammal BPI is 0.25 and the fossil mammal is 0.27. The cynodont BPI is significantly closer to the reptile mean value (Fig. 3). As overall carbonate content is deduced from BPI, a similar result was obtained, as the cynodont carbonate percentage weight (mean 6.13%) significantly differs from that of the mammals (3.2%) (independent 1-tailed *t*-test: $t_s = 8.464$; $df = 9$; $P < 0.05$) and closely resembles the *Crocodylus niloticus* and *Varanus* value (mean 6.32%).

These differences between extant and fossil enamel are likely due to a rearrangement of the various ions in the fossil material. However, it was expected that the cynodont BAI would be closer to the fossil mammal BAI than the extant reptile results as these study genera represent derived cynodonts. When considering both BAI and BPI, the cynodont values clearly group with the reptile results and not with the mammalian peak ratios (Fig. 3). Although the *Diademodon* BAI is slightly higher than the rest of the fossil BAI (Table 2), it also groups with the reptile BAI peak ratios (Fig. 3). As the cynodont PCI falls between the mammalian and reptile PCI peak ratios, it is possible that an increase in PCI occurred during fossilization. If the reason for the cynodont and reptile enamel structure similarity is biological, then the cynodont PCI peak ratio is to be expected. The cynodont enamel may have been poorly crystalline, similar to that of reptiles, and the increase in PCI may have occurred during fossilization.

Although diagenesis cannot be entirely excluded, the cynodont spectra profiles in our study indicate that the biological apatite is reasonably well preserved. Significantly, we find that there is a clear distinction between the mammal (extant and fossil) and cynodont peak ratios. If these observations are a true reflection of cynodont enamel structure, this observation has implications for the pathways of cynodont enamel mineralization. The cynodonts acquired increasingly mammalian morphological characteristics during their evolution, including their gross dental structure. However, the derived cynodonts exhibit nonprismatic enamel, which is similar to extant reptiles [14, 15]. Although it has yet to be concluded if the presence of enamel prisms is associated with mammalian physiological processes, together with the results in this study it suggests that cynodont enamel structure was not mammal-like. Our results emphasize the point that cynodonts had a combination of both reptilian and mammalian traits. Much emphasis is put on the mammalian morphological characteristics in the cynodonts. However, these animals evidently had features from both groups and their biology is unlikely to have been identical to either group.

Conclusion

The similarity in BPI and carbonate content between the extant reptile and cynodont enamel may indicate a similarity in structural properties. As cynodont dentition was becoming increasingly mammal-like [4, 12, 31], it is expected that the cynodont enamel structure would have closely resembled extant mammalian enamel. However, the results in this study suggest that cynodont apatite structure may have been more similar to that of reptiles than to mammals.

This study is the first to conduct FTIR spectroscopy on such old fossil enamel material (approximately 220 million years old, Early Triassic [32]) and has demonstrated the potential for examining the structural changes that occur in therapsid enamel during fossilization. Further research is still required to shed more light on therapsid enamel and its similarities/differences with extant mammals.

References

1. Hopson JA (1987) The mammal-like reptiles. A study of transitional fossils. Am Biol Teacher 49:16–26
2. Rubidge BS, Sidor CA (2001) Evolutionary patterns among Permo-Triassic therapsids. Ann Rev Ecol Syst 32:449–480
3. Jenkins FA (1971) The postcranial skeleton of African cynodonts. Problems in the early evolution of the mammalian postcranial skeleton. Buletin of the Peabody Museum of Natural History, 36: 1–216,
4. Kemp TS (1982) Mammal-like reptiles and the origin of mammals. Academic Press, London
5. Sidor CA, Hopson JA (1998) Ghost lineages and 'mammalness': assessing the temporal pattern of character acquisition in the Synapsida. Paleobiology 24:254–273
6. Luo Z-X, Crompton AW, Sun A-L (2001) A new mammaliaform from the Early Jurassic of China and evolution of mammalian characteristics. Science 292:1535–1540
7. Sidor CA (2001) Simplification as a trend in synapsid cranial evolution. Evolution 55:1419–1442
8. Blob RW (2001) Evolution of hindlimb posture in non-mammalian therapsids: biomechanical tests of paleontological hypotheses. Paleobiology 27:14–38
9. Botha J, Chinsamy A (2000) Growth patterns deduced from the bone histology of the cynodonts *Diademodon* and *Cynognathus*. J Vert Paleontol 204:705–711
10. Hopson JA (1971) Postcanine replacement in the gomphodont cynodont *Diademodon*. Zool J Linn Soc 50:1–21
11. Grine FE (1976) Postcanine (gomphodont) tooth wear in the mammal-like reptile *Diademodon:* a scanning electron microscope (SEM) study. Proc Electron Microsc Soc S Afr 6:51–52
12. Grine FE (1977) Postcanine tooth function and jaw movement in the gomphodont cynodont *Diademodon* (Reptilia; Therapsida). Palaeontol Afr 20:123–135

13. Grine FE (1978) Postcanine dental structure in the mammal-like reptile *Diademodon* (Therapsida; Cynodontia). Proc Electron Microsc Soc S Afr 8:123–124

14. Grine FE, Vrba ES, Cruickshank ARI (1979) Enamel prisms and diphyodonty: linked apomorphies of Mammalia. S Afr J Sci 75:114–120

15. Wood CB, Stern DN (1995) The first prismatic enamel in reptiles and mammals: latest evidence for prisms as a synapomorphy of Mammalia. J Vert Paleontol 15(3 Suppl): 6–61A

16. Wood CB, Werth AJ, Shah-hosseini S (1999) Enamel Hunter–Schreger bands in *Inia* (Odontoceti) and *Basilosaurus* (Archaeoceti)—Functional versus phylogenetic influences. J Vert Paleontol 19(3 Suppl):85A

17. LeGeros RZ (1991) Calcium phosphates in oral biology and medicine. Karger, New York

18. Rey C, Renugopalakrisrman V, Shimizu M, Collins B, Glimcher MJ (1991) A resolution-enhanced Fourier Transform Infrared spectroscopic study of the environment of the CO_3^{2-} ion in the mineral phase of enamel during its formation and maturation. Calcif Tissue Int 49:259–268

19. Michel V, Ildefonse P, Morin G (1995) Chemical and structural changes in *Cervus elaphus* tooth enamels during fossilization (Lazaret cave): a combined IR and XRD Rietveld analysis. Appl Geochem 10:145–159

20. Sponheimer M, Lee–Thorp JA (1999) Alteration of enamel carbonate environments during fossilization. J Archaeol Sci 26:143–150

21. Hassan A (1977) Mineralogical studies of bone apatite and their implications for radiocarbon dating. Radiocarbon 193:364–374

22. Brink AS (1956) Speculations on some advanced mammalian characteristics in the higher mammal-like reptiles. Palaeontol Afr 4:77–96

23. Seeley HG (1908) On the dentition of the palate in the South African fossil reptile genus *Cynognathus*. Geol Mag 5:486–491

24. Broom R (1911) On the structure of the skull in cynodont reptiles. Proc Zool Soc Lond 11:900–905

25. Gregory WK, Camp CL (1918) Reconstruction of the skeleton of *Cynognathus*. Bull Am Mus Nat Hist 38:538–544

26. Seeley HG (1895) Researches on the structure, organization and classification of the fossil Reptilia. On *Diademodon*. Philos Trans R Soc Lond B Biol Sci 185:1029–1041

27. Watson DMS (1911) The skull of *Diademodon* with notes on those of some other cynodonts. Ann Mag Nat Hist 8:295–330

28. Brink AS (1955) A study on the skeleton of *Diademodon*. Palaeontol Afr 3:3–39

29. Hopson JA (1994) Synapsid evolution and the radiation of non-eutherian mammals. In: Prothero DRP, Schoch RM (Eds.) Major features of vertebrate evolution. Paleontological Society, Knoxville TN, pp 190–219

30. Seeley HG (1895) On the structure, organization and classification of the fossil Reptilia III. On *Trirachodon*. Philos Trans R Soc Lond B Biol Sci 186:48–57

31. Hopson JA (1991) Convergence in mammals, tritheledonts, and tritylodonts. J Vert Paleontol 11(3 Suppl):36A

32. Harland WB, Armstrong RL, Cox AV, Craig LE, Smith AG, Smith DG (1990) A geologic time scale. Cambridge University Press, Cambridge